EUROPEAN ORGANIZATION FOR NUCLEAR RESEARCH

Proposal to the ISOLDE and Neutron Time-of-Flight Committee

Determination of the B(E3,0^+->3^-) strength in the octupole correlated nucleus ^{144}Ba using Coulomb excitation

6/10/2011

M. Scheck[1], D.T. Joss[2], M. Albers[3], A. Andreyev[4], C. Barton[5], A. Blazhev[3], T. Bloch[1], S. Bönig[1], P.A. Butler[2], J. Cederkäll[6], D. Cline[7], T.E. Cocolios[8], J. Diriken[9], P. Van Duppen[9], L.P. Gaffney[2], R. Gernhäuser[10], A. Görgen[11], T. Grahn[12], M. Guttormsen[11], K. Hadynska Klek[12], A. Hayes[7], R.-D. Herzberg[2], M. Huyse[9], A. Ignatov[1], T. Ilieva[1], J. Iwanicki[12], D.G. Jenkins[5], J. Jolie[3], R. Julin[13], N. Kesteloot[9], T. Kröll[1], R. Krücken[10], E. Kwan[14], A.-C. Larsen[11], M.T. McEllistrem[15], K. Moschner[3], D. Mücher[10], P. Napiorkowski[12], K. Nowak[10], R.D. Page[2], J. Pakarinen[8], D. Pietak[12], D. Radeck[3], G. Rainovski[16], P. Reiter[3], M. von Schmid[1], M. Seidlitz[3], S. Siem[11], G.S. Simpson[17], J. Srebrny[12], P. Thirolf[18], M. Thürauf[1], D. Voulot[8], R. Wadsworth[5], N. Warr[3], F. Wenander[8], K.Wimmer[19], K. Wrzosek-Lipska[9], C.-Y. Wu[14], S.W. Yates[15], and M. Zielinska[20]

[1] TU Darmstadt
[2] University of Liverpool
[3] University of Cologne
[4] University of the West of Scotland
[5] University of York
[6] Lund University
[7] University of Rochester
[8] CERN-ISOLDE
[9] KU Leuven
[10] TU München
[11] University of Oslo
[12] HIL University of Warsaw
[13] University of Jyväskylä
[14] Lawrence Livermore Laboratory
[15] University of Kentucky
[16] Sofia University
[17] LPSC Grenoble
[18] LMU München
[19] NSCL Michigan State University
[20] CEA Saclay

CERN-INTC-2011-039 / INTC-P-305
05/10/2011

Spokesperson(s): M.Scheck (mscheck@ikp.tu-darmstadt.de)
D.T.Joss (dtj@ns.ph.liv.ac.uk)
Local contact: J.Pakarinen (janne.pakarinen@cern.ch)

Abstract

We propose to exploit the unique capability of ISOLDE to provide intense post-accelerated ^{144}Ba ion beams from the REX facility to enable the Coulomb excitation of the first 3^- state in this nucleus. By measuring the γ-ray yields of the E1 decay connecting the 3^- and 2^+ states using the MINIBALL array, we can obtain the interesting $<3^-|E3|0^+>$ transition matrix element. The result will give quantitative information about octupole correlations in this nucleus. We require **27 shifts** to fulfil the aims of the experiment.

Requested shifts: 27 shifts, (split into 1 runs over 1 years)

Physics Case

There is considerable theoretical and experimental evidence that atomic nuclei can assume reflection asymmetric shapes, which arise from the octupole degree of freedom [1]. From a microscopic point of view, the wave functions of low-lying 3^- octupole excitations must contain components which include the intruding, unique-parity subshell nlj. Because of the nature of the octupole-octupole interaction in nuclei, octupole correlations arise when this intruder state comes close to the Fermi level, giving rise to [(n+1)(l-3)(j-3), nlj] particle-hole configurations (e.g. [$2d_{5/2}$, $1h_{11/2}$] or [$2f_{7/2}$, $1i_{13/2}$]) at relatively low excitation energies. The strongest correlations occur near the proton numbers Z= 34, 56, and 88 and the neutron numbers N= 34, 56, 88, and 134. Indeed, at these values of Z and N nuclei exhibit phenomena associated with reflection asymmetry such as odd-even staggering of the positive and negative parity yrast bands in even-even nuclei and parity doublets in odd mass nuclei, see e.g. [2,3], and enhanced E1 moments due to a division of the centre-of-charge and centre-of-mass [4].

An inverse sum rule for the octupole excitations is plotted in Figure 1. The inverse sum rule was chosen, as it forces octupole excitations originating from particle-hole excitations over a shell closure to scale down with their comparably high excitation energies. Figure 1 illustrates that an unambiguous and direct evidence for enhanced octupole correlations in these nuclei is provided by a combination of the excitation energy E_3 and the M(E3) =

$<3^-|E3|0^+>$ transition matrix element [6,7].

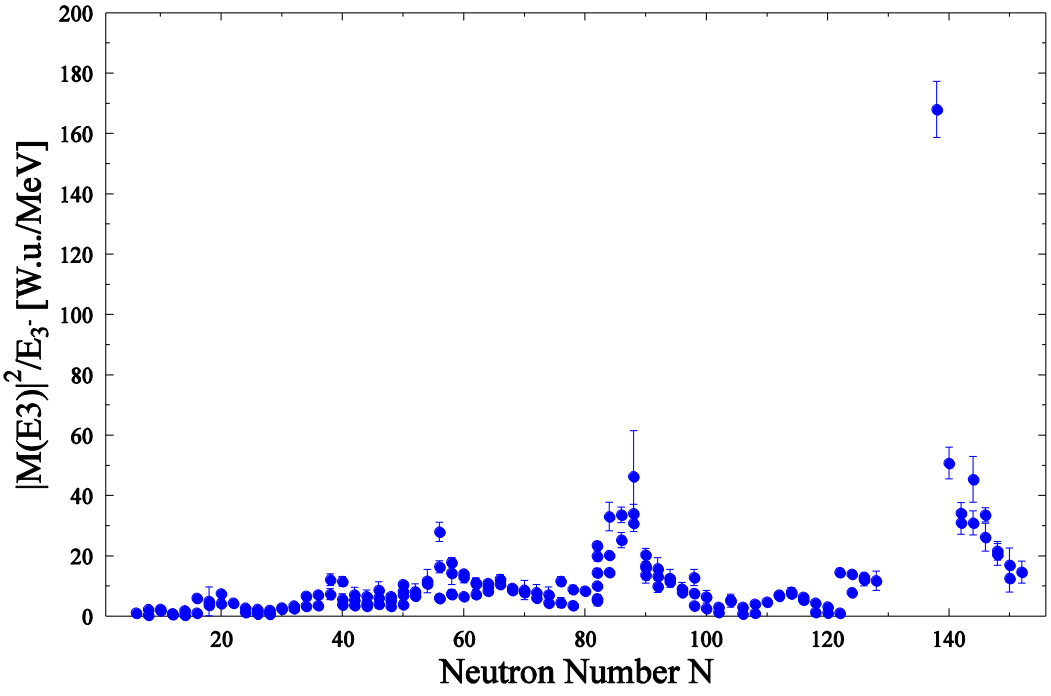

Figure 1: Plot of the inverse sum rule $|M(E3)|^2/E_3$ as a function of the neutron number N (data taken from [5]).

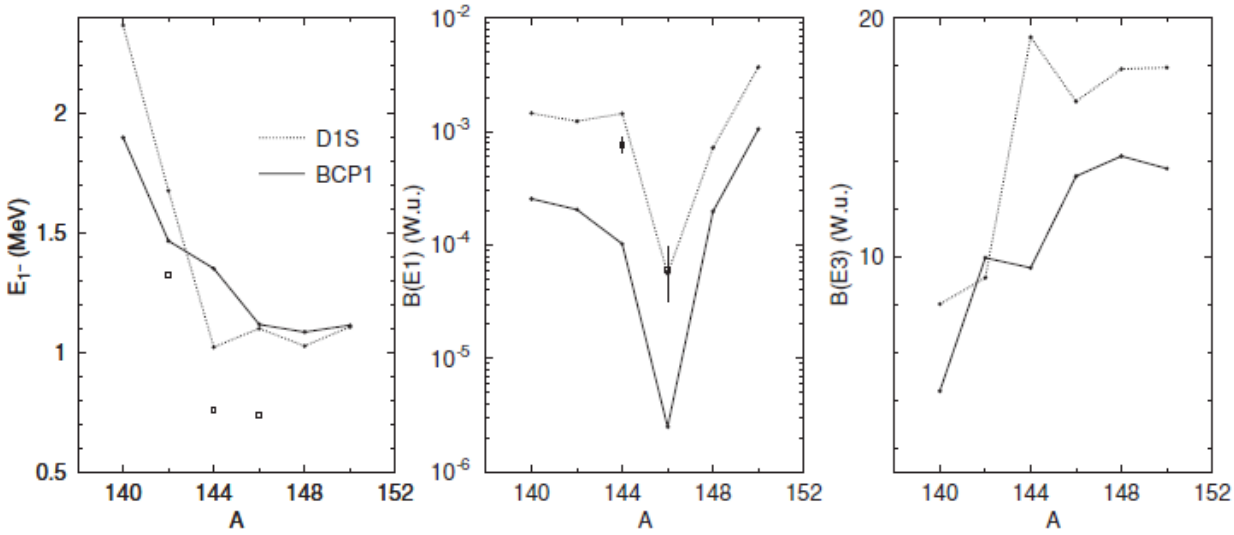

Figure 2: Observables related to the octupole degree of freedom for the Ba isotopic chain as predicted by the BCP density functional theory (solid lines) and the HFB mean-field method using the Gogny D1S interaction (figure taken from [9]). Shown are the excitation energy of 1- state, the B(E1, 1- -> 0+) and the B(E3, 3- -> 0+) reduced transition probabilities.

Pronounced octupole correlations are clearly visible in the vicinity of the octupole magic numbers. The octupole collectivity in the region near Z=88 and N=134 is already under investigation by our collaboration using Coulomb excitation at REX-ISOLDE (IS475) [8]. The second octupole soft region accessible with the beam energies, currently, provided by REX is the region near the nucleon numbers Z=56 and N=88.

A large number of theoretical approaches (a broad overview is given in reference [1]), such as in the Nilsson-Strutinsky approach with deformed folded Yukawa and Woods-Saxon potentials, cluster models, and self-consistent models using the Skyrme and Gogny forces were developed to describe the experimental features associated with strong octupole correlations. Recently, Robledo and co-workers used the Barcelona-Catania-Paris energy density functionals to describe octupole correlations in the Barium isotopic chain and compared the results to a Hartee Fock Bogoliubov (HFB) calculation performed with the Gogny D1S interaction [9]. HFB mean-field calculations are a well-established theoretical tool to study octupole correlations (e.g. see refs. [10,11]). The predictions of the two approaches deviate most for ^{144}Ba. For this particular nucleus the B(E3) strength deviates by a factor of two and the B(E1) strength even by an order of magnitude (see Fig. 2). The differences of the two approaches extend to their predictions for the degree of octupole correlations found in the ground state of the neutron-rich Ba isotopes. While the density functional theory approach does not exhibit a minimum of the Potential Energy Curve as function of the octupole moment Q_3 at values other than zero, the HFB approach predicts for ^{144,146,148}Ba a minimum at non-zero Q_3 values. Here, the minimum is most pronounced for ^{144}Ba. However, one has to point out, that the minimum is not well pronounced. The maximum depth of only 0.7 MeV, found for ^{144}Ba, is still rather small compared to the typical energy of an octupole vibration.

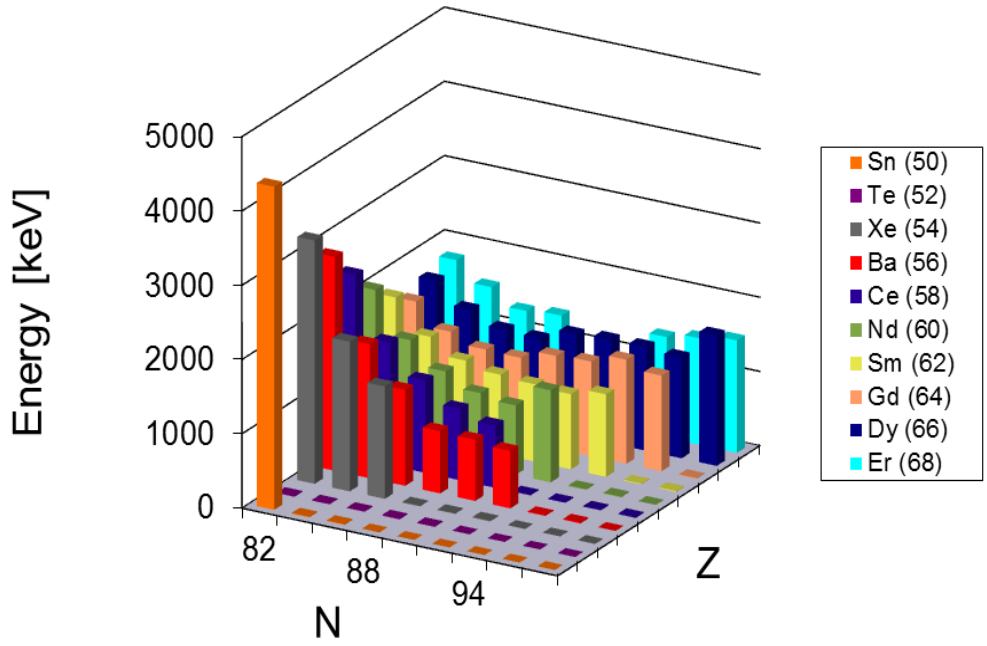

Figure 2: Plot of the excitation energies, E_3, of the first excited 3^- states in the A~130-170 mass region (data taken from [8]).

Evidence for a stronger quadrupole deformation of the odd-spin negative parity band in ^{144}Ba is given by larger in-band B(E2) values measured using the Differential Decay Curve Method (DDCM) [12]. The observed behaviour was explained within a cluster model that assumes an intrinsic octupole deformation, but also with a quadrupole-octupole coupled model assuming no intrinsic octupole deformation.

As pointed out earlier, related to the reflection asymmetric pear shape associated with a strongly octupole correlated nucleus is a staggering of odd- and even-parity yrast states. As illustrated in Figure 5, the level scheme of ^{144}Ba exhibits this feature at comparably low spins (J>6). A rather exotic approach [13] in a liquid drop like model describes the observed spin-dependent transition from an octupole vibrator to a rotational system by octupole tidal waves aligning at a critical rotational frequency.

The excitation energies of the first excited 3^- state in the A~130-170 mass region, as known so far, are plotted in Figure 3. Here, the Ba isotopic chain exhibits the lowest excitation energies in this particular region.

Until now, experiments to measure reliable B(E3) data in the A~140-150 mass region were only feasible for the stable isotopes. However, within the past few years Coulomb excitation experiments on heavy nuclei have become standard at the REX-ISOLDE facility. Within our experimental programme to investigate strongly octupole correlated nuclei in the A ~ 222 mass region, we were able to demonstrate the feasibility of observing Coulomb excitation of negative parity via E3-excitation paths using post-accelerated radioactive ion

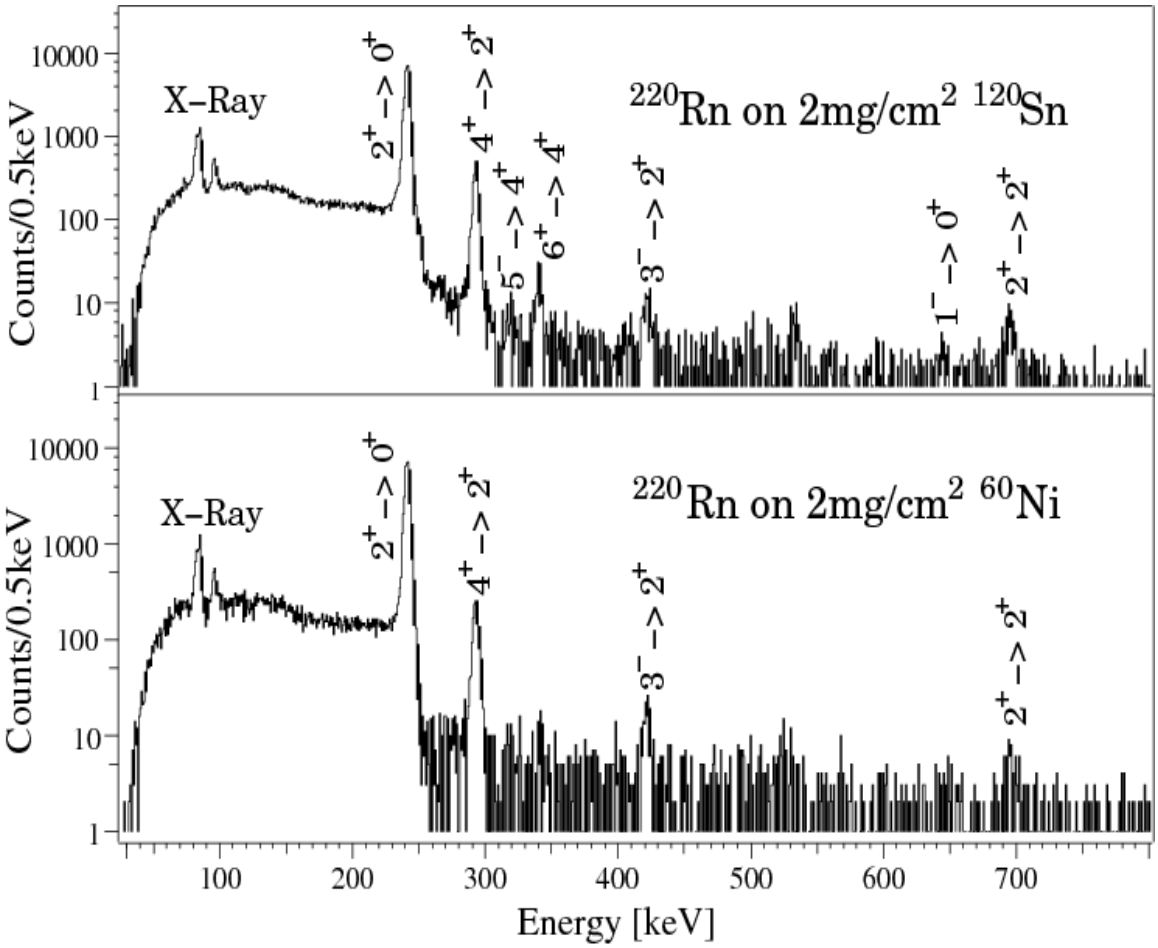

Figure 4: Spectra of ^{220}Rn Coulomb excited by a ^{120}Sn target (top panel) and ^{60}Ni (bottom panel) as recorded in the IS475 campaign. The 423-keV peak of the 3^- -> 2^+ transition is clearly visible in both spectra. Please note the change in two-step excitation, recognizable by comparing the 4^+ -> 2^+ peak in the two spectra.

beams provided by REX-ISOLDE. Spectra obtained in this campaign are shown in Figure 4. In the upper panel the spectrum of ^{220}Rn Coulomb excited on a 2 mg/cm^2 ^{120}Sn target is shown. The spectrum contains several peaks identified as transitions of ^{220}Rn. In the lower panel the spectrum of ^{220}Rn Coulomb excited on a ^{60}Ni target is shown. In both spectra the 423-keV peak, belonging to the 3^- -> 2^+ transition, depopulating the Coulomb excited 3^- state, is clearly visible. In the spectrum recorded with the ^{60}Ni target, the reduced intensity of the 4^+ -> 2^+ decay, in comparison to the 2^+ -> 0^+ transition, of the two-step excited 4^+ state indicates the decrease of two-step excitation probability when using a target with a lower Z. Since the analysis of a Coulomb excitation experiments aims to solve a complex network of many linked matrix elements, a sufficient set of experimental data is needed to have fully determined variables. This is especially true for the Coulomb excitation of negative parity states, where for most transitions E1 and E3 matrix elements have to be considered. In order to obtain a sufficient number of observables (γ-ray yields), we need to change the experimental conditions (Coulomb excitation paths) for the scattering process by using targets with different proton numbers.

Experimental set-up and Coulex yields

ISOLDE is unique world-wide in having the capability of providing sufficient accelerated beam intensity [14] of the ^{144}Ba isotope for a Coulomb excitation experiment. The competing CARIBU facility at Argonne National Laboratories [15] is, so far, not capable of producing and post-accelerating the beam of interest with a purity and an intensity sufficient to perform Coulomb excitation experiments. Similarly the Holifield Facility at Oak Ridge National Laboratory cannot produce sufficient yield of accelerated Ba ions.

Since the lifetimes of the positive parity states are well known, the first excited 2^+ state within an accuracy of 3% [12,16,17,18], we are able to normalize the Coulomb excitation of the negative parity states relative to them. Essentially, this means no purification of the beam using the ISOLDE standard Laser ON/OFF technique in order to obtain the target excitation relative to the beam of interest is necessary. Nevertheless, as in previous measurements of the neutron-rich Ba isotopes at REX-ISOLDE [19] contaminants in the beam were observed, we will have to check if a transition stemming from an isobaric contaminant is contributing to one of the peaks of interest. If this would be the case, enough statistics is required to be able to subtract the background spectrum from the spectrum of interest. According to the data base [18] none of the possible even-even isobaric contaminants has transitions overlapping with the transitions of interest for us. However, this is not guaranteed for the odd-odd isobars. The laser ionization scheme available for the Ba isotopes indicates a laser-ionization efficiency between 10 and 15% [20]. The use of the laser system has two advantages. First it will, additional to the already large fraction of surface ionized atoms, further increase the Ba available for post acceleration and second we can, when subtracting the spectrum recorded in the laser ON mode from the spectra recorded in the laser OFF mode, check for contaminants. Furthermore, if it is necessary, we can subtract the spectrum recorded in laser OFF mode from the spectrum recorded in laser ON mode and obtain a purified Ba spectrum. The primary production yields and ion yields following charge breeding and post-acceleration are presented in Table 1.

Nucleus	**Half-life** [s]	**Target Material**	**I_p** [μA]	**PSB or SC**	**ISOLDE production yield** [Ions/μC]	**Yield at the Coulex target** [Ions/s]
^{144}Ba	11.5	UC_X	1.5	SC	1.0×10^7	2.0×10^5

Table 1: Production yield of ^{144}Ba as found in reference [14]. For the number of ions at the secondary Coulex target we assume 2% transmission efficiency through REX-ISOLDE.

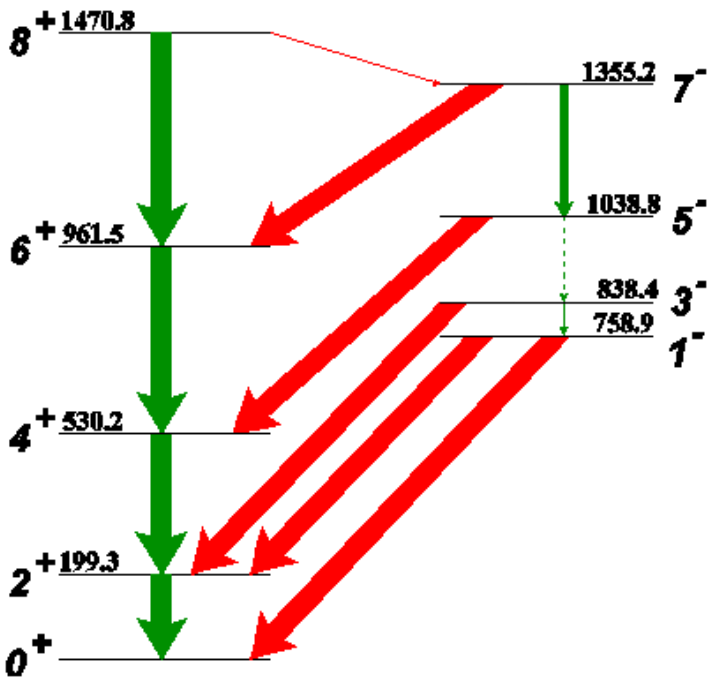

Figure 5: Low-lying, low-spin level scheme of ^{144}Ba as relevant to subbarrier Coulomb excitation. The thickness of the arrows is proportional to the relative γ-ray intensities. The data are taken from reference [18].

The low-energy level scheme of ^{144}Ba [18] relevant to sub-barrier Coulomb studies is shown in Figure 5. The primary aim of this experiment is to determine the E3 matrix element between the ground state and the first excited 3^- state that will give direct information about octupole correlations in this nucleus. Coulomb excitation will excite in a first order process the first excited 2^+ and 3^- states via E2 and E3 transitions, respectively. Excitations via E1 transitions are usually orders of magnitude less probable. In addition, the 1^- and 3^- states will be excited by E2xE3 second order processes via the 2^+ state. Since the population of the 1^- level exclusively happens as two-step excitation, the relation of the γ-decay yields of the 1^- and the 3^- states contains the information about the probability for one-step and two-step excitation of the negative parity levels. The first 4^+ state will be excited in a second-order process involving the first 2^+ state. We intend to use a combination of the low-Z target ^{12}C and the high-Z target ^{60}Ni. The combination of the Carbon and Nickel data sets will yield enough information to disentangle the one-step and multi-step excitation paths unambiguously and, therefore, will allow for a precise determination of the B(E3) strength. The kinematics expected for a Coulomb excitation process by scattering ^{144}Ba projectiles on a 2mg/cm^2 ^{60}Ni target is shown in Figure 6.

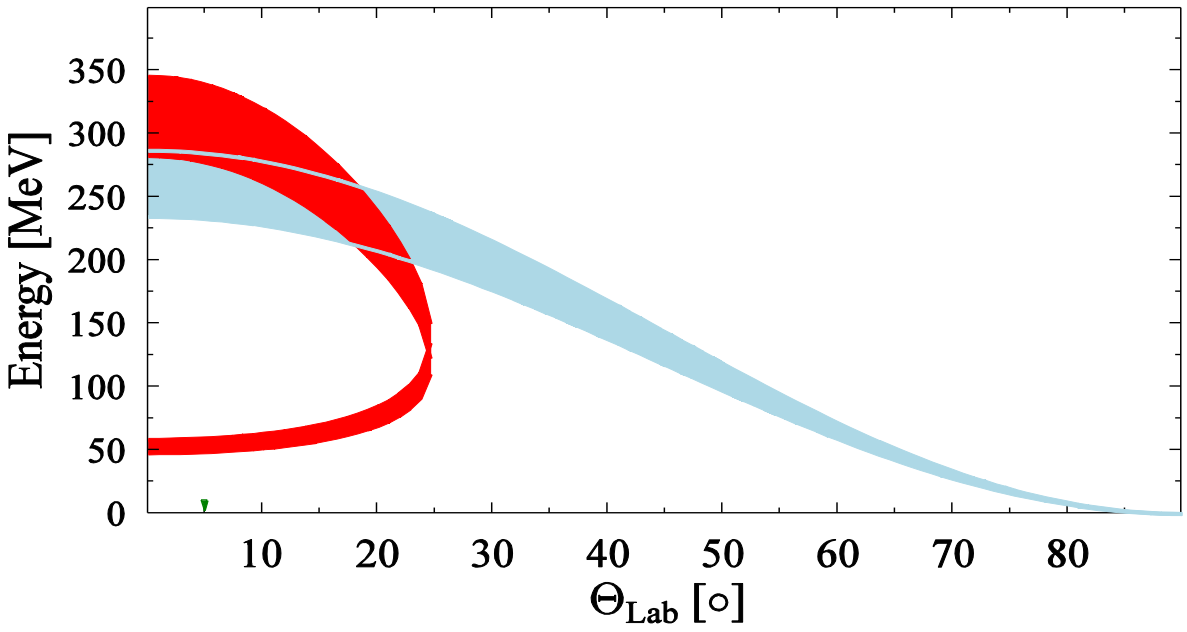

Figure 6: Kinematics of the Coulomb excitation reaction of ^{144}Ba scattered by a 2 mg/cm^2 ^{60}Ni target. The red band corresponds to the scattered projectiles and the light blue band to the scattered target recoils. The width of the bands corresponds to a 10% relative resolution of the particle detector. Please note, that the minimum angle detectable with the T-Rex scattering chamber [22] is 15°.

In the proposed experiment, the Ba beams will undergo excitation using ^{12}C and ^{60}Ni secondary targets. The de-excitation γ-rays will be observed using the MINIBALL array containing 8 triple clusters of 6-fold segmented Ge detectors [21]. The detector array has an efficiency of 7% for 1.3 MeV photons. The scattered target recoils will be detected using the T-Rex scattering chamber [22] covering laboratory angles in a range between 15° and 165°. The Coulex □-ray yields for a 2.85 MeV/u ^{144}Ba beam onto 2 mg/cm^2 ^{12}C and ^{60}Ni targets were calculated with the computer code GOSIA [23]. For the calculations a total □-ray detection efficiency of 10% was assumed. The <(J+2)|E2|J> transition matrix elements were calculated using the lifetime values found in [16,17,18]. For the 7^- state the lifetime obtained in [13] was used. For the states, where no lifetimes are known, we used the same tendency of the <(J+2)|E2|J> transition matrix elements as observed for ^{148}Nd [6] relative to the states where values are published. For the <J+1|E1|J> transition matrix elements we used a constant value as calculated from the lifetime values of the 7^- and 9^- states published in [13]. For the <J|E2|J> diagonal matrix elements we used the values as published for ^{148}Nd [5]. The <J+3|E3|J> and <J+1|E3|J> matrix elements were calculated assuming an E3 strength of 15 W.u. for these transitions. The corresponding □-ray yields calculated using the Coulomb excitation analysis code GOSIA are presented in Table 2. For the Carbon target no projectiles will be scattered in the angular range covered by the particle detector (>15°). Therefore, the yields for the Carbon target were calculated for target-recoil detection in the angular range covered by the particle detector. As illustrated in Figure 6, for the Nickel target the distribution of scattered projectiles and target recoils overlaps in the

angular range covered by the particle detector. Thus, projectile gating is only possible for high centre-of-mass angles for which the number of scattered projectiles is low. Consequently, the yields were calculated for target-recoil detection with scattering angles larger than 25°.

Target	Beam time [h]	Transition	Transition energy [keV]	γ-ray yields [Counts]
^{12}C	**80**	$2^+_1 \rightarrow 0^+_1$	199.3	66510
		$4^+_1 \rightarrow 2^+_1$	330.9	150
		$6^+_1 \rightarrow 4^+_1$	431.3	<10
		$3^-_1 \rightarrow 2^+_1$	639.0	150
		$1^-_1 \rightarrow 0^+_1$	759.0	60
^{60}Ni	**80**	$2^+_1 \rightarrow 0^+_1$	199.3	163040
		$4^+_1 \rightarrow 2^+_1$	330.9	5280
		$6^+_1 \rightarrow 4^+_1$	431.3	120
		$3^-_1 \rightarrow 2^+_1$	639.0	140
		$1^-_1 \rightarrow 0^+_1$	759.0	90

Table 2: Estimated γ-ray yields following the Coulomb excitation of 2.85 MeV/u ^{144}Ba on a 2 mg/cm^2 secondary target. The yields estimates are calculated for target-recoil detection. For further details of the calculation, see text.

Note that radiation protection issues [24] due to the presence of the long-living isobar ^{144}Ce ($T_{1/2}$ = 284.8d) in the decay chain has been considered. The long half-life of ^{144}Ce will result in a low specific activity. Thus, the addition to the overall activity is negligible.

Summary of requested shifts:

We estimate that **10 shifts** will be sufficient for yield measurements of transitions in ^{144}Ba Coulomb excited by ^{12}C, **10 shifts** for the ^{58}Ni secondary target, as well as **3 shifts** for setting up REX. In addition, **4 shifts** in Laser Off mode are required to determine the relative intensity of transitions stemming from odd-odd isobars, eventually overlapping with transitions of ^{144}Ba. The intended program will be sufficient to determine the B(E3, 0^+ -> 3) strength with less than 15 % relative error. In total **27 shifts** are requested.

References:

[1] P. A. Butler and W. Nazarewicz, (1996) Rev. Mod. Phys. **68**, No.2, 349

[2] J. F. C. Cocks *et al.*, (1997) Phys. Rev. Lett. **78**, 2920 ; (1999) Nucl. Phys A **645**, 61

[3] M Dahlinger et al., (1988) Nucl. Phys. **A484**, 337

[4] P. A. Butler and W. Nazarewicz, (1991) Nucl. Phys. **A533** 249

[5] T. Kibédi and R. H. Spear, (2002) Atomic Data and Nuclear Data Tables **80**, 35

[6] R.Ibbotson et al., (1993) Phys. Rev. Lett. **71** 1990

[7] H. J. Wollersheim *et al.*, (1993) Nucl. Phys **A556**, 261

[8] CERN-INTC-2008-021; INTC-P-244 (Spokespersons M. Scheck and P.A. Butler)

[9] L. M. Robledo et al., (2010) Phys. Rev. C **81**, 034315

[10] J. L. Egido and L. M. Robledo, (1989) Nucl. Phys. **A494**, 85

[11] E. Garrotte, J. L. Egido and L. M. Robledo, (1997) Phys. Lett. B**410**, 86

[12] T. M. Shneidman et al., (2005) Eur. Phys. J. A **25**, 387-396

[13] S. Frauendorf, (2008) Phys. Rev. C **77**, 021304 (R)

[14] http://isolde.web.cern.ch/ISOLDE/

[15] G. Savard and R. Pardo, Proposal for the ^{252}Cf source upgrade to the ATLAS facility

[16] D. C. Biswas et al., (2005) Phys. Rev. C **71**, 011301 (R)

[17] R. Krücken et al., (2001) Phys. Rev. C **64**, 017305

[18] http://www.nndc.bnl.gov/endsf

[19] CERN-INTC-2002-015; INTC-P-156 (Spokespersons D. Habs and Th. Kröll)

[20] V. Fedosseev, private communication

[21] J. Eberth *et al.*, (2001) Prog. Part. Nucl. Phys. **46**, 389

[22] V. Bildstein et al., (2007) Prog. Part. Nucl. Phys. **59**, 386

[23] T. Czosnyka, D. Cline, and C. Y. Wu, http://www.pas.rochester.edu/~cline/Research/Gosia.htm

[24] F. Wenander, private communication

Appendix

DESCRIPTION OF THE PROPOSED EXPERIMENT

The experimental setup comprises: *(name the fixed-ISOLDE installations, as well as flexible elements of the experiment)*

Part of the Choose an item.	Availability	Design and manufacturing
MINIBALL + T-REX	☒ Existing	☒ To be used without any modification
[Part 1 of experiment/ equipment]	☐ Existing	☐ To be used without any modification ☐ To be modified
	☐ New	☐ Standard equipment supplied by a manufacturer ☐ CERN/collaboration responsible for the design and/or manufacturing
[Part 2 experiment/ equipment]	☐ Existing	☐ To be used without any modification ☐ To be modified
	☐ New	☐ Standard equipment supplied by a manufacturer ☐ CERN/collaboration responsible for the design and/or manufacturing
[insert lines if needed]		

HAZARDS GENERATED BY THE EXPERIMENT

(if using fixed installation) Hazards named in the document relevant for the fixed [COLLAPS, CRIS, ISOLTRAP, MINIBALL + only CD, MINIBALL + T-REX, NICOLE, SSP-GLM chamber, SSP-GHM chamber, or WITCH] installation.

Additional hazards:

Hazards			
	[Part 1 of the experiment/equipment]	*[Part 2 of the experiment/equipment]*	*[Part 3 of the experiment/equipment]*
Thermodynamic and fluidic			
Pressure	[pressure][Bar], [volume][l]		
Vacuum			
Temperature	[temperature] [K]		
Heat transfer			
Thermal properties of materials			
Cryogenic fluid	[fluid], [pressure][Bar], [volume][l]		
Electrical and electromagnetic			
Electricity	[voltage] [V], [current][A]		
Static electricity			
Magnetic field	[magnetic field] [T]		
Batteries	☐		
Capacitors	☐		
Ionizing radiation			
Target material	[material]		
Beam partide type (e, p, ions, etc)			

Beam intensity			
Beam energy			
Cooling liquids	[liquid]		
Gases	[gas]		
Calibration sources:	☐		
• Open source	☐		
• Sealed source	☐ [ISO standard]		
• Isotope			
• Activity			
Use of activated material:			
• Description	☐		
• Dose rate on contact and in 10 cm distance	[dose] [mSV]		
• Isotope			
• Activity			
Non-ionizing radiation			
Laser			
UV light			
Microwaves (300MHz-30 GHz)			
Radiofrequency (1-300MHz)			
Chemical			
Toxic	[chemical agent], [quantity]		
Harmful	[chemical agent], [quantity]		
CMR (carcinogens, mutagens and substances toxic to reproduction)	[chemical agent], [quantity]		
Corrosive	[chemical agent], [quantity]		
Irritant	[chemical agent], [quantity]		
Flammable	[chemical agent], [quantity]		
Oxidizing	[chemical agent], [quantity]		
Explosiveness	[chemical agent], [quantity]		
Asphyxiant	[chemical agent], [quantity]		
Dangerous for the environment	[chemical agent], [quantity]		
Mechanical			
Physical impact or mechanical energy (moving parts)	[location]		
Mechanical properties (Sharp, rough, slippery)	[location]		
Vibration	[location]		
Vehicles and Means of Transport	[location]		
Noise			
Frequency	[frequency], [Hz]		
Intensity			
Physical			
Confined spaces	[location]		
High workplaces	[location]		
Access to high workplaces	[location]		
Obstructions in passageways	[location]		
Manual handling	[location]		
Poor ergonomics	[location]		

0.1 Hazard identification

3.2 Average electrical power requirements (excluding fixed ISOLDE-installation mentioned above): *(make a rough estimate of the total power consumption of the additional equipment used in the experiment)*